



CERN-EP-2022-264
21 November 2022

Enhanced deuteron coalescence probability in jets

ALICE Collaboration

Abstract

The transverse-momentum (p_T) spectra and coalescence parameters B_2 of (anti)deuterons are measured in pp collisions at $\sqrt{s} = 13$ TeV in and out of jets. In this measurement, the direction of the leading particle with the highest p_T in the event ($p_T^{\text{lead}} > 5$ GeV/c) is used as an approximation for the jet axis. The event is consequently divided into three azimuthal regions and the jet signal is obtained as the difference between the Toward region, that contains jet fragmentation products in addition to the underlying event (UE), and the Transverse region, which is dominated by the UE. The coalescence parameter in the jet is found to be approximately a factor of 10 larger than that in the underlying event. This experimental observation is consistent with the coalescence picture and can be attributed to the smaller average phase-space distance between nucleons in the jet cone as compared to the underlying event. The results presented in this Letter are compared to predictions from a simple nucleon coalescence model, where the phase space distributions of nucleons are generated using PYTHIA 8 with the Monash 2013 tuning, and to predictions from a deuteron production model based on ordinary nuclear reactions with parametrized energy-dependent cross sections tuned on data. The latter model is implemented in PYTHIA 8.3. Both models reproduce the observed large difference between in-jet and out-of-jet coalescence parameters.

arXiv:2211.15204v1 [nucl-ex] 28 Nov 2022

The production mechanisms of light (anti)nuclei in high-energy hadronic collisions is still unclear and currently under intense debate in the scientific community, despite the plethora of results published in recent years at different collision energies, ranging from the AGS [1–4], to the SPS [5], RHIC [6–11], and the LHC [12–27]. The experimental data are typically described using two different phenomenological approaches: the baryon coalescence approach and the statistical hadronization model (SHM). In the coalescence model [28–34], multi-baryon states are assumed to be formed by coalescence of baryons that are close in phase space at kinetic freeze-out (occurring when the elastic scatterings among the particles produced in the collision cease). In the simple coalescence approach [29], only momentum correlations are considered, while in state-of-the-art implementations [30], the quantum-mechanical properties of baryons and bound states are taken into account and the coalescence probability is calculated from the overlap between the phase space distributions of individual (point-like) baryons and the Wigner density of the final-state cluster. The phase space distributions of nucleons at freeze-out are generated using general-purpose Monte Carlo (MC) event generators or relativistic hydrodynamical simulations [31, 35]. In the SHM [36–43], light (anti)nuclei, as well as other hadron species, are assumed to be emitted by a source in local thermal and hadrochemical equilibrium with their abundances being fixed at chemical freeze-out (occurring when the inelastic scatterings stop). The grand-canonical approach provides an excellent description of the measured hadron yields in central nucleus–nucleus collisions, in which a large number of particles is produced, ranging from few hundreds to 2000 charged particles per unit of rapidity with increasing collision energy [40]. For small systems, such as those produced in proton–proton (pp) and proton–nucleus collisions, the production of light nuclei can be described using a different implementation of this model based on the canonical ensemble, where exact conservation of quantum numbers is required [43]. Significant deviations in this case are observed between the experimental data and the predictions from the canonical SHM [24]. The study of the production mechanisms of multi-baryon bound states in high-energy hadronic collisions is one of the goals of the experimental program of ALICE.

Measurements of light (anti)nuclei produced at accelerators are also important for indirect dark matter (DM) searches as they provide input for the estimates of the background of antinuclei produced in space. Several experiments, such as AMS-02 [44] and GAPS [45], are searching for antinuclei [46, 47], but, so far, only antiprotons have been detected in space [48]. The possible presence of antinuclei in our Galaxy could be explained either by reactions of cosmic rays (CRs) with the interstellar medium (ISM) or by decays/annihilations of dark matter candidates. Both CRs and the ISM mostly consist of hydrogen (90%), helium (8%), and only in small percentage of heavier nuclei [49]. Hence, most of the relevant collisions for the production of CR antinuclei in the Galaxy are pp, p– ^4He and ^4He –p. Antinuclei are produced if the center-of-mass energy per nucleon–nucleon collision ($\sqrt{s_{\text{NN}}}$) of such collisions is above a given energy threshold, which is 6 GeV for antideuterons and 8 GeV for anti- ^3He , for instance. Hence, one of the goals of the existing experimental programs at different accelerator facilities is to pin down the microscopic production process of antinuclei in hadronic collisions or DM decay, such to be able to correctly interpret the future measurements in space.

Further insight into the (anti)nuclei production mechanisms can be obtained by measuring their production in and out of jets in pp collisions. Hadrons in the jet cone are closer in phase space compared to hadrons out of the jet. In a jet fragmentation, the produced particles are strongly correlated in phase space, i.e., particles which are close in space have also similar momenta [50, 51]. In the coalescence picture, this condition should result in a larger coalescence probability in jets compared to that out of jets, since the proximity in both space and momentum is required for coalescence. Hence, the probability of coalescence in jets is increased with respect to that in the UE, where space and momentum are not correlated, i.e., close-by particles can have very different momenta and vice-versa. The coalescence probability can be quantified by the coalescence parameter B_A , defined, in the case of deuterons, as the ratio between the invariant yield of the deuterons and the square of the invariant yield of protons:

$$B_2 = \left(\frac{1}{2\pi p_T^d} \frac{d^2 N_d}{dy dp_T^d} \right) / \left(\frac{1}{2\pi p_T^p} \frac{d^2 N_p}{dy dp_T^p} \right)^2, \quad (1)$$

where the labels d and p indicate the deuteron and the proton, respectively, and $p_T^p = p_T^d/2$, assuming that protons and neutrons have the same production spectra, since they belong to the same isospin doublet.

Deuteron production in jets has already been measured in pp collisions at $\sqrt{s} = 13$ TeV by the ALICE Collaboration using the two-particle correlation method [22]. The p_T spectrum of (anti)deuterons in the jet is found to be consistent with predictions based on the PYTHIA 8 event generator [52] coupled to a simple coalescence afterburner [53]. In the latter, deuteron formation is assumed to happen if a proton and a neutron have a momentum difference $\Delta p < p_0$, with $p_0 = 110$ MeV/c, thus ignoring the space coordinates in the calculation of the coalescence probability. It was also concluded that the yield of deuterons in jets, in events with a leading particle with $p_T > 5$ GeV/c at midrapidity, is about 10% of that in the underlying event (UE).

This study is expanded in this Letter and complemented by the first measurement of (anti)deuteron coalescence parameters in and out of jets. The direction of a leading particle with high transverse-momentum ($p_T^{\text{lead}} > 5$ GeV/c) at midrapidity is used as an approximation for the jet axis. The p_T spectra and coalescence parameters of (anti)deuterons are measured in three different azimuthal regions defined based on $\Delta\phi = |\phi_d - \phi_{\text{lead}}|$, where ϕ_d is the azimuthal angle of the deuterons and ϕ_{lead} is that of the leading particle. The three 120°-wide azimuthal regions and the corresponding $\Delta\phi$ intervals are the same as those defined in Refs. [54, 55]: the one around the leading particle (Toward, $|\Delta\phi| < 60^\circ$), the one back-to-back to it (Away, $|\Delta\phi| > 120^\circ$), and the one transverse to both of them (Transverse, $|\Delta\phi| < 120^\circ$). The Toward and Away regions contain contributions from the leading and recoil jets in addition to the underlying event, while the Transverse region is dominated by the underlying event.

A detailed description of the ALICE apparatus and its performance can be found in Refs. [56] and [57]. Trajectories of charged particles are reconstructed in the ALICE central barrel with the Inner Tracking System (ITS) [56] and the Time Projection Chamber (TPC) [58], which cover the full azimuthal angle and the pseudorapidity interval $|\eta| < 0.9$. These are located within a large solenoidal magnet, providing a highly homogeneous magnetic field of 0.5 T parallel to the beam line. The TPC provides up to 159 spatial points per track for charged-particle reconstruction and particle identification (PID) through the measurement of the specific ionization energy loss dE/dx in the gas volume. The PID is complemented by the Time-Of-Flight (TOF) system [59] located at a radial distance of 3.7 m from the nominal interaction point. It measures the arrival time of particles relative to the event collision time provided by the TOF detector itself or by the T0 detectors, two arrays of Cherenkov counters located at forward and backward rapidities ($4.6 < \eta < 4.9$ and $-3.3 < \eta < -3.0$) [57, 60].

The data used for this analysis were collected in 2016, 2017, and 2018 during the LHC pp runs at $\sqrt{s} = 13$ TeV. A minimum bias (MB) event trigger was used, which requires coincident signals in the V0 detectors (two plastic scintillator arrays located at forward and backward rapidities, $2.8 < \eta < 5.1$ and $-3.7 < \eta < -1.7$ [61]) synchronous with the bunch crossing time defined by the LHC clock. Events with multiple collision vertices, reconstructed from track segments in the two innermost layers of the ITS, are tagged as pile-up and removed from the analysis [57]. A total of approximately 1.7 billion MB pp events are considered for further analysis, corresponding to an integrated luminosity of about 30 nb⁻¹. Events with at least one charged primary particle with $p_T > 5$ GeV/c are selected, which correspond to approximately 1% of the MB pp collisions.

Deuteron candidates are selected from charged-particle tracks reconstructed in the ITS and TPC in the pseudorapidity interval $|\eta| < 0.8$. Basic track quality criteria are applied, e.g., selecting on the number of space points associated to the track in the TPC and ITS and on the χ^2 of the track fit, as done in previous light (anti)nucleus analyses, such as in Ref. [20]. The track selection criteria used for the leading particle

are the same as in Ref. [54].

(Anti)deuterons are identified in the rapidity interval $|y| < 0.5$ in the range $0.6 < p_T < 1.2$ GeV/ c by requiring that their energy loss per unit of track length measured by the TPC is within $3\sigma_{dE/dx}$ from the expected average for (anti)deuterons, where $\sigma_{dE/dx}$ is the dE/dx resolution. For $1.2 < p_T < 3.0$ GeV/ c , the particle identification is complemented by the TOF and the (anti)deuteron signal is extracted from a fit to the $n\sigma_{\text{TOF}} = (\Delta t - \Delta t_d)/\sigma_{\text{TOF}}$ distribution, where Δt is the measured time-of-flight, Δt_d its expected value for deuterons and σ_{TOF} the resolution on the time-of-flight measurement. The fit function consists of a Gaussian with an exponential tail on the right side for the signal and the sum of two exponential functions for the background [13]. The signal is extracted by integrating the signal function in the asymmetric interval $[\mu_0 - 3\sigma_{\text{TOF}}, \mu_0 + 3.5\sigma_{\text{TOF}}]$, where μ_0 is the mean of the Gaussian function.

The raw (anti)deuteron p_T spectra are corrected for the reconstruction efficiency and, only for deuterons, for the fraction of secondary deuterons produced by spallation in interactions between primary particles and the detector material. This correction is based on fits to the distance of closest approach (DCA) of the deuteron track to the primary vertex using template distributions extracted from MC simulations, as described in Refs. [20, 21, 23]. Both corrections are calculated using MC simulations in which (anti)nuclei are embedded into pp collision events generated using PYTHIA 8.1 with the Monash 2013 tune [62]. (Anti)nuclei are generated with uniform p_T and rapidity distributions within $0 < p_T < 10$ GeV/ c and $-1 < y < 1$. The passage of particles through the ALICE detector is simulated using GEANT4 [63]. The reconstruction efficiency is calculated as the ratio of the number of reconstructed and generated (anti)deuterons in the simulation, after the proper re-weighting of the generated p_T distribution according to the Levy-Tsallis function. The same track selection and PID criteria as those used in data are applied. The fraction of secondary deuterons is approximately 0.5 in the lowest p_T interval ($0.6 < p_T < 0.8$ GeV/ c) and decreases exponentially with increasing p_T , becoming negligible for $p_T > 1.6$ GeV/ c . The fraction of secondary deuterons is weakly dependent on the azimuthal region.

The dominant contributions to the systematic uncertainties are related to the track selection, the particle identification, the limited knowledge of the ALICE material budget, the uncertainties on the hadronic interaction cross section of (anti)deuterons, and the procedure used to estimate the fraction of secondary nuclei. The uncertainty related to the track selection is estimated by repeating the analysis using different track selection criteria and considering the RMS of the distribution of the results in each p_T interval. This contribution is found to range between 8 (1)% and 6 (5)% for deuterons (antideuterons), depending on p_T . Such uncertainty is larger for deuterons at low p_T , due to the DCA cut variations which are sensitive to the secondary nuclei. The PID uncertainty is estimated by varying the (anti)deuteron selection criteria in the TPC and TOF, the fit functions, and the signal extraction strategy (bin counting or integral of the fit function). The PID systematic uncertainty rises with p_T , from 4% to 8%. The systematic uncertainty due to the estimate of the primary fraction correction is obtained by varying the histogram bin width and the fit range of the fits to the DCA distributions. This contribution depends on the azimuthal region, and it ranges between 14% (10% and 7%) and few percent for the Away region (Toward and Transverse, respectively). The contribution from ITS–TPC and TPC–TOF matching efficiencies are estimated from charged particle tracks by comparing the probabilities of prolonging a track from the TPC to the ITS (TOF) in data and MC [20]. The uncertainty is approximately 2% for the ITS–TPC matching efficiency and 5% for the TPC–TOF one, weakly dependent on p_T . The uncertainty on the material budget (1%) is taken from Ref. [20]. The uncertainty on the hadronic interaction cross section of (anti)deuterons is estimated by varying the default inelastic cross section of (anti)deuterons in GEANT4 by the uncertainties of the measurements [49, 64–67] and is $\sim 1\%$ (3%) for deuterons (antideuterons). The total uncertainty is obtained as the quadratic sum of each individual contribution and is found to be about 10%.

The average of the deuteron and antideuteron p_T distributions measured in the three azimuthal regions discussed above, are shown in Fig. 1 left. Individual Lévy-Tsallis fits [68] are also shown. The p_T spectrum of (anti)deuterons in jets is obtained by subtracting the spectrum in the Transverse region,

dominated by the underlying event, from that in the Toward region, which contains contributions from both jet fragmentation and the underlying event. In the subtraction, the systematic uncertainties are treated as independent, to be conservative. The resulting spectrum, with a much harder shape compared to the UE spectrum, is shown in Fig. 1 right, with squared markers, and compared to the in-jet deuteron spectrum measured with the two-particle correlation method taken from Ref. [22]. Excellent agreement is found between the deuteron p_T spectra in jets obtained with the two methods, proving the validity of the subtraction method to obtain the deuteron spectrum in jets. These results confirm that the integrated yield of deuterons in jets, in events with $p_T^{\text{lead}} > 5 \text{ GeV}/c$ at midrapidity, is only roughly 10% of that in the UE, as already pointed out in Ref. [22].

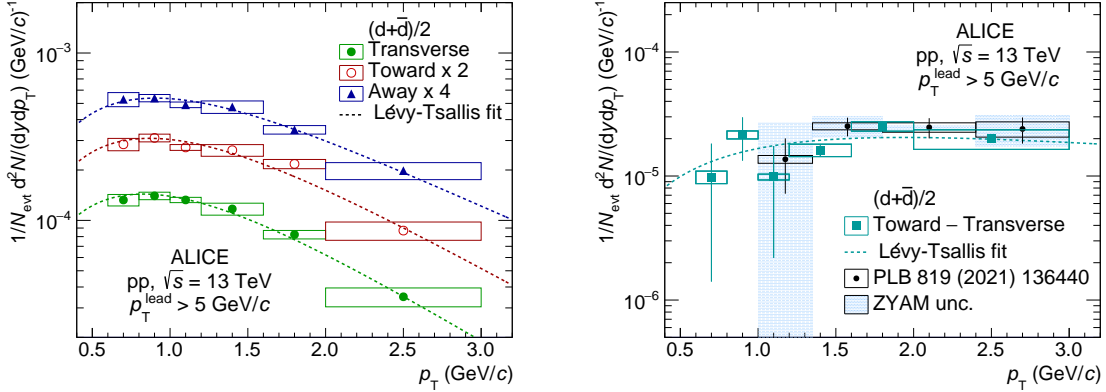


Figure 1: Average of deuteron and antideuteron p_T -differential yields in the three azimuthal regions (on the left) and in jets (on the right), measured in pp collisions at $\sqrt{s} = 13 \text{ TeV}$. Statistical and systematic uncertainties are represented by vertical bars and boxes, respectively. On the right, shaded (blue) boxes show the uncertainty on the results from Ref. [22] related to the subtraction of the uncorrelated background using the ZYAM method [69]. Individual Lévy-Tsallis fits are also shown.

The coalescence parameters in the jet (B_2^{Jet}) and underlying event (B_2^{UE}) are calculated using Eq. 1. The spectra for (anti)protons are derived from the R_T -differential p_T spectra published in Ref. [70], integrating over the full R_T , which is the underlying event activity classifier defined as $R_T = N_T^{\text{ch}} / \langle N_T^{\text{ch}} \rangle$ (N_T^{ch} being the charged-particle multiplicity measured in the Transverse region and $\langle N_T^{\text{ch}} \rangle$ its average) [54]. The p_T spectrum of (anti)protons in jets is obtained by subtracting the efficiency-corrected p_T spectra in the Transverse region from those in the Toward region taken from Ref. [70], as done for deuterons. The coalescence parameters B_2^{Jet} and B_2^{UE} are shown in Fig. 2 as a function of the transverse momentum per nucleon, p_T/A . The coalescence parameter B_2^{Jet} is found to be about a factor of 10 larger compared to that in the underlying event. Hence, despite the limited contribution of nuclei arising from jets to their total production yield, the probability that two nucleons in the jet cone coalesce into a deuteron is enhanced with respect to the corresponding coalescence probability in the underlying event. This experimental observation can be interpreted, within the coalescence model, as due to the reduced distance in phase space between nucleons in the jets compared to those in the underlying event.

These results are compared to predictions from simple coalescence and reaction-based deuteron production models. In the former approach, the phase space distributions of nucleons are generated with PYTHIA 8 with the Monash 2013 tune [62] and their p_T spectra are re-weighted to match the proton p_T spectra measured by ALICE in the three different azimuthal regions [70]. Spatial correlations are ignored and deuteron formation is assumed to happen if a proton and a neutron have a momentum difference below a given coalescence momentum $\Delta p < p_0$ in the deuteron rest frame. The best estimate of the coalescence momentum, for this model, is $p_0 = 285 \pm 1 \text{ MeV}/c$. A detailed description of these coalescence calculations can be found in Ref. [71].

In the reaction-based model [72], (anti)deuterons are generated by ordinary nuclear reactions between

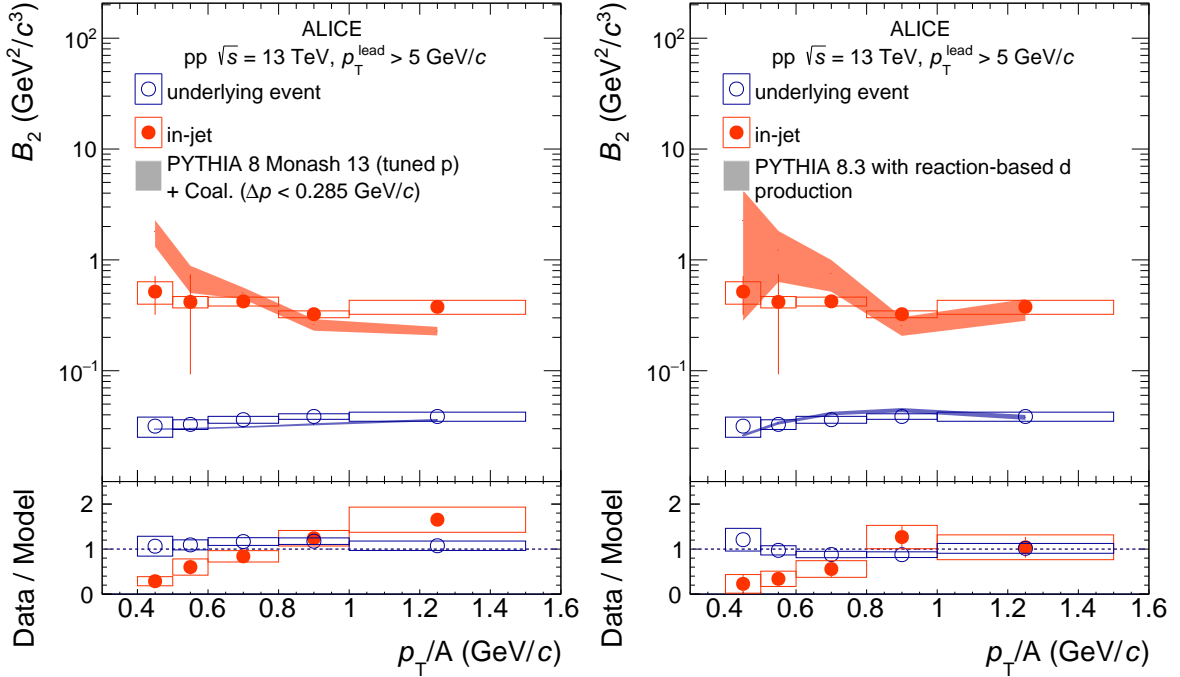


Figure 2: Coalescence parameter in jets, B_2^{Jet} , and in the underlying event, B_2^{UE} , as a function of p_T/A in comparison with the predictions from PYTHIA 8 with the Monash 2013 tune with a coalescence afterburner (left panel) and the reaction-based PYTHIA 8.3 model (right panel).

nucleons produced in the collision with parameterized energy-dependent cross sections tuned on available experimental data [73]. The following nuclear reactions are considered: $p + n \rightarrow \gamma + d$, $p + n \rightarrow \pi^0 + d$, $p + n \rightarrow \pi^0 + \pi^0 + d$, $p + n \rightarrow \pi^+ + \pi^- + d$, $p + p \rightarrow \pi^+ + d$, $p + p \rightarrow \pi^+ + \pi^0 + d$, $n + n \rightarrow \pi^- + d$, $n + n \rightarrow \pi^- + \pi^0 + d$. Such a model is implemented in the MC event generator PYTHIA 8.3. Both simple coalescence and the reaction-based model are based on the assumption that coalescence can happen only if protons and neutrons are close in phase space. However, there are two main differences between the models. The first concerns the p_0 cut off which is introduced as a step function in the coalescence model, while in PYTHIA 8.3 the deuteron formation happens according to the differential cross section of the reactions listed above. The second difference is related to the kinematics of the process: in the coalescence model the deuteron four-momentum is given by the sum of the proton and neutron four-momenta, while in the reaction-based model, part of the initial four-momentum is carried away by the pion(s) or photon according to energy and momentum conservation rules. The uncertainties of the coalescence model are discussed in Ref. [71], while for PYTHIA 8.3 only statistical uncertainties are shown.

As shown in Fig. 2, both models provide good qualitative descriptions of the data. In particular, they are capable of reproducing the observed large difference between B_2^{Jet} and B_2^{UE} . While the p_T/A dependence of B_2^{UE} is well described by both approaches within the uncertainties, the observed nearly-flat trend of B_2^{Jet} is not reproduced by the models, which instead give a decreasing trend with increasing p_T/A and overestimate the B_2^{Jet} for low p_T/A .

The results presented in this Letter indicate for the first time an enhanced deuteron coalescence probability in jets compared to the underlying event. This enhancement, of a factor ~ 10 , is measured with a good precision and a huge significance. This experimental observation is a parameter-free and absolute prediction of coalescence, which decisively proves the formation of bound states by coalescence when nucleons have a smaller average phase-space distance, as it is the case in the jet cone. This study will be extended to heavier (anti)nuclei, such as (anti) ^3He , and to p–Pb collisions, with the LHC Run 3 data. Further investigations of the coalescence parameters B_A in the jet and in the underlying event, in small

collision systems, which reproduce the CRs interactions originating nuclei in our Galaxy, will provide additional insight into the production mechanisms and will contribute to further constrain the coalescence models. These studies will be crucial to correctly interpret any future measurement of antinuclei in satellite and balloon-borne experiments in space.

References

- [1] **E878** Collaboration, M. J. Bennett *et al.*, “Light nuclei production in relativistic Au + nucleus collisions”, *Phys. Rev. C* **58** (1998) 1155–1164.
- [2] **E802** Collaboration, L. Ahle *et al.*, “Proton and deuteron production in Au + Au reactions at 11.6 A-GeV/c”, *Phys. Rev. C* **60** (1999) 064901.
- [3] **E864** Collaboration, T. A. Armstrong *et al.*, “Measurements of light nuclei production in 11.5 A-GeV/c Au + Pb heavy ion collisions”, *Phys. Rev. C* **61** (2000) 064908, arXiv:nuc1-ex/0003009.
- [4] **E864** Collaboration, T. A. Armstrong *et al.*, “Anti-deuteron yield at the AGS and coalescence implications”, *Phys. Rev. Lett.* **85** (2000) 2685–2688, arXiv:nuc1-ex/0005001.
- [5] **NA52 (NEWMASS)** Collaboration, G. Ambrosini *et al.*, “Baryon and anti-baryon production in lead-lead collisions at 158 A GeV/c”, *Phys. Lett. B* **417** (1998) 202–210.
- [6] **STAR** Collaboration, C. Adler *et al.*, “Antideuteron and anti-³He production in $\sqrt{s_{NN}} = 130$ GeV Au+Au collisions”, *Phys. Rev. Lett.* **87** (2001) 262301, arXiv:nuc1-ex/0108022. [Erratum: Phys.Rev.Lett. 87, 279902 (2001)].
- [7] **PHENIX** Collaboration, S. S. Adler *et al.*, “Deuteron and antideuteron production in Au + Au collisions at 200 GeV”, *Phys. Rev. Lett.* **94** (2005) 122302, arXiv:nuc1-ex/0406004.
- [8] **BRAHMS** Collaboration, I. Arsene *et al.*, “Rapidity dependence of deuteron production in Au+Au collisions at $\sqrt{s_{NN}} = 200$ GeV”, *Phys. Rev. C* **83** (2011) 044906, arXiv:1005.5427 [nuc1-ex].
- [9] **STAR** Collaboration, H. Agakishiev *et al.*, “Observation of the antimatter helium-4 nucleus”, *Nature* **473** (2011) 353, arXiv:1103.3312 [nuc1-ex]. [Erratum: Nature 475 (2011) 412].
- [10] **STAR** Collaboration, L. Adamczyk *et al.*, “Measurement of elliptic flow of light nuclei at $\sqrt{s_{NN}} = 200, 62.4, 39, 27, 19.6, 11.5, \text{ and } 7.7$ GeV at the BNL Relativistic Heavy Ion Collider”, *Phys. Rev. C* **94** (2016) 034908, arXiv:1601.07052 [nuc1-ex].
- [11] **STAR** Collaboration, J. Adam *et al.*, “Beam energy dependence of (anti-)deuteron production in Au + Au collisions at the BNL Relativistic Heavy Ion Collider”, *Phys. Rev. C* **99** (2019) 064905, arXiv:1903.11778 [nuc1-ex].
- [12] **ALICE** Collaboration, J. Adam *et al.*, “Precision measurement of the mass difference between light nuclei and anti-nuclei”, *Nature Phys.* **11** (2015) 811–814, arXiv:1508.03986 [nuc1-ex].
- [13] **ALICE** Collaboration, J. Adam *et al.*, “Production of light nuclei and anti-nuclei in pp and Pb–Pb collisions at energies available at the CERN Large Hadron Collider”, *Phys. Rev. C* **93** (2016) 024917, arXiv:1506.08951 [nuc1-ex].
- [14] **ALICE** Collaboration, S. Acharya *et al.*, “Multiplicity dependence of (anti-)deuteron production in pp collisions at $\sqrt{s} = 7$ TeV”, *Phys. Lett. B* **794** (2019) 50–63, arXiv:1902.09290 [nuc1-ex].

- [15] ALICE Collaboration, S. Acharya *et al.*, “Measurement of deuteron spectra and elliptic flow in Pb–Pb collisions at $\sqrt{s_{NN}} = 2.76$ TeV at the LHC”, *Eur. Phys. J. C* **77** (2017) 658, arXiv:1707.07304 [nucl-ex].
- [16] ALICE Collaboration, S. Acharya *et al.*, “Production of deuterons, tritons, ^3He nuclei and their antinuclei in pp collisions at $\sqrt{s} = 0.9, 2.76$ and 7 TeV”, *Phys. Rev. C* **97** (2018) 024615, arXiv:1709.08522 [nucl-ex].
- [17] ALICE Collaboration, S. Acharya *et al.*, “Production of ^4He and $^4\overline{\text{He}}$ in Pb–Pb collisions at $\sqrt{s_{NN}} = 2.76$ TeV at the LHC”, *Nucl. Phys. A* **971** (2018) 1–20, arXiv:1710.07531 [nucl-ex].
- [18] ALICE Collaboration, S. Acharya *et al.*, “Multiplicity dependence of light (anti-)nuclei production in p–Pb collisions at $\sqrt{s_{NN}} = 5.02$ TeV”, *Phys. Lett. B* **800** (2020) 135043, arXiv:1906.03136 [nucl-ex].
- [19] ALICE Collaboration, S. Acharya *et al.*, “Production of (anti-) ^3He and (anti-) ^3H in p–Pb collisions at $\sqrt{s_{NN}} = 5.02$ TeV”, *Phys. Rev. C* **101** (2020) 044906, arXiv:1910.14401 [nucl-ex].
- [20] ALICE Collaboration, S. Acharya *et al.*, “(Anti-)deuteron production in pp collisions at $\sqrt{s} = 13$ TeV”, *Eur. Phys. J. C* **80** (2020) 889, arXiv:2003.03184 [nucl-ex].
- [21] ALICE Collaboration, S. Acharya *et al.*, “Production of light (anti)nuclei in pp collisions at $\sqrt{s} = 13$ TeV”, *JHEP* **01** (2022) 106, arXiv:2109.13026 [nucl-ex].
- [22] ALICE Collaboration, S. Acharya *et al.*, “Jet-associated deuteron production in pp collisions at $\sqrt{s} = 13$ TeV”, *Phys. Lett. B* **819** (2021) 136440, arXiv:2011.05898 [nucl-ex].
- [23] ALICE Collaboration, S. Acharya *et al.*, “Production of light (anti)nuclei in pp collisions at $\sqrt{s} = 5.02$ TeV”, *Eur. Phys. J. C* **82** (2022) 289, arXiv:2112.00610 [nucl-ex].
- [24] ALICE Collaboration, S. Acharya *et al.*, “Hypertriton Production in p–Pb Collisions at $\sqrt{s_{NN}}=5.02$ TeV”, *Phys. Rev. Lett.* **128** (2022) 252003, arXiv:2107.10627 [nucl-ex].
- [25] ALICE Collaboration, S. Acharya *et al.*, “Measurement of deuteron spectra and elliptic flow in Pb–Pb collisions at $\sqrt{s_{NN}} = 2.76$ TeV at the LHC”, *Eur. Phys. J. C* **77** (2017) 658, arXiv:1707.07304 [nucl-ex].
- [26] ALICE Collaboration, S. Acharya *et al.*, “Elliptic and triangular flow of (anti)deuterons in Pb–Pb collisions at $\sqrt{s_{NN}} = 5.02$ TeV”, *Phys. Rev. C* **102** (2020) 055203, arXiv:2005.14639 [nucl-ex].
- [27] ALICE Collaboration, S. Acharya *et al.*, “Measurement of the (anti-) ^3He elliptic flow in Pb–Pb collisions at $\sqrt{s_{NN}} = 5.02$ TeV”, *Phys. Lett. B* **805** (2020) 135414, arXiv:1910.09718 [nucl-ex].
- [28] S. T. Butler and C. A. Pearson, “Deuterons from High-Energy Proton Bombardment of Matter”, *Phys. Rev.* **129** (1963) 836–842.
- [29] J. I. Kapusta, “Mechanisms for deuteron production in relativistic nuclear collisions”, *Phys. Rev. C* **21** (1980) 1301–1310.
- [30] R. Scheibl and U. W. Heinz, “Coalescence and flow in ultrarelativistic heavy ion collisions”, *Phys. Rev. C* **59** (1999) 1585–1602, arXiv:nucl-th/9809092 [nucl-th].

- [31] W. Zhao, L. Zhu, H. Zheng, C. M. Ko, and H. Song, “Spectra and flow of light nuclei in relativistic heavy ion collisions at energies available at the BNL Relativistic Heavy Ion Collider and at the CERN Large Hadron Collider”, *Phys. Rev.* **C98** (2018) 054905, arXiv:1807.02813 [nucl-th].
- [32] K. Blum and M. Takimoto, “Nuclear coalescence from correlation functions”, *Phys. Rev. C* **99** (2019) 044913, arXiv:1901.07088 [nucl-th].
- [33] K.-J. Sun, C. M. Ko, and B. Dönigus, “Suppression of light nuclei production in collisions of small systems at the Large Hadron Collider”, *Phys. Lett.* **B792** (2019) 132–137, arXiv:1812.05175 [nucl-th].
- [34] M. Kachelrieß, S. Ostapchenko, and J. Tjemsland, “Alternative coalescence model for deuteron, tritium, helium-3 and their antinuclei”, *Eur. Phys. J. A* **56** (2020) 4, arXiv:1905.01192 [hep-ph].
- [35] D. Oliinychenko, L.-G. Pang, H. Elfner, and V. Koch, “Microscopic study of deuteron production in Pb–Pb collisions at $\sqrt{s_{NN}} = 2.76$ TeV via hydrodynamics and a hadronic afterburner”, *Phys. Rev. C* **99** (2019) 044907, arXiv:1809.03071 [hep-ph].
- [36] J. Cleymans, S. Kabana, I. Kraus, H. Oeschler, K. Redlich, and N. Sharma, “Antimatter production in proton-proton and heavy-ion collisions at ultrarelativistic energies”, *Phys. Rev.* **C84** (2011) 054916, arXiv:1105.3719 [hep-ph].
- [37] A. Andronic, P. Braun-Munzinger, J. Stachel, and H. Stöcker, “Production of light nuclei, hypernuclei and their antiparticles in relativistic nuclear collisions”, *Phys. Lett.* **B697** (2011) 203–207, arXiv:1010.2995 [nucl-th].
- [38] F. Becattini, E. Grossi, M. Bleicher, J. Steinheimer, and R. Stock, “Centrality dependence of hadronization and chemical freeze-out conditions in heavy ion collisions at $\sqrt{s_{NN}} = 2.76$ TeV”, *Phys. Rev.* **C90** (2014) 054907, arXiv:1405.0710 [nucl-th].
- [39] V. Vovchenko and H. Stöcker, “Examination of the sensitivity of the thermal fits to heavy-ion hadron yield data to the modeling of the eigenvolume interactions”, *Phys. Rev.* **C95** (2017) 044904, arXiv:1606.06218 [hep-ph].
- [40] A. Andronic, P. Braun-Munzinger, K. Redlich, and J. Stachel, “Decoding the phase structure of QCD via particle production at high energy”, *Nature* **561** (2018) 321–330, arXiv:1710.09425 [nucl-th].
- [41] N. Sharma, J. Cleymans, B. Hippolyte, and M. Paradzka, “A Comparison of p-p, p-Pb, Pb-Pb Collisions in the Thermal Model: Multiplicity Dependence of Thermal Parameters”, *Phys. Rev.* **C99** (2019) 044914, arXiv:1811.00399 [hep-ph].
- [42] V. Vovchenko, B. Dönigus, and H. Stoecker, “Canonical statistical model analysis of p-p, p-Pb, and Pb-Pb collisions at energies available at the CERN Large Hadron Collider”, *Phys. Rev. C* **100** (2019) 054906, arXiv:1906.03145 [hep-ph].
- [43] V. Vovchenko, B. Dönigus, and H. Stoecker, “Multiplicity dependence of light nuclei production at LHC energies in the canonical statistical model”, *Phys. Lett. B* **785** (2018) 171–174, arXiv:1808.05245 [hep-ph].
- [44] A. Kounine, “The Alpha Magnetic Spectrometer on the International Space Station”, *Int. J. Mod. Phys. E* **21** (2012) 1230005.

- [45] C. J. Hailey, “An indirect search for dark matter using antideuterons: the GAPS experiment”, *New J. Phys.* **11** (2009) 105022.
- [46] F. Donato, N. Fornengo, and D. Maurin, “Antideuteron fluxes from dark matter annihilation in diffusion models”, *Phys. Rev.* **D78** (2008) 043506, arXiv:0803.2640 [hep-ph].
- [47] M. Korsmeier, F. Donato, and N. Fornengo, “Prospects to verify a possible dark matter hint in cosmic antiprotons with antideuterons and antihelium”, *Phys. Rev.* **D97** (2018) 103011, arXiv:1711.08465 [astro-ph.HE].
- [48] AMS Collaboration, M. Aguilar *et al.*, “Antiproton Flux, Antiproton-to-Proton Flux Ratio, and Properties of Elementary Particle Fluxes in Primary Cosmic Rays Measured with the Alpha Magnetic Spectrometer on the International Space Station”, *Phys. Rev. Lett.* **117** (2016) 091103.
- [49] ALICE Collaboration, S. Acharya *et al.*, “Measurement of the low-energy antideuteron inelastic cross section”, *Phys. Rev. Lett.* **125** (2020) 162001, arXiv:2005.11122 [nucl-ex].
- [50] R. D. Field and R. P. Feynman, “A Parametrization of the Properties of Quark Jets”, *Nucl. Phys. B* **136** (1978) 1.
- [51] B. Andersson, G. Gustafson, G. Ingelman, and T. Sjostrand, “Parton Fragmentation and String Dynamics”, *Phys. Rept.* **97** (1983) 31–145.
- [52] T. Sjostrand, S. Mrenna, and P. Z. Skands, “A Brief Introduction to PYTHIA 8.1”, *Comput. Phys. Commun.* **178** (2008) 852–867, arXiv:0710.3820 [hep-ph].
- [53] ALICE Collaboration, S. Acharya *et al.*, “Supplemental material: afterburner for generating light (anti-)nuclei with QCD-inspired event generators in pp collisions”, *ALICE-PUBLIC-2017-010* (Sep, 2017). <https://cds.cern.ch/record/2285500>.
- [54] ALICE Collaboration, S. Acharya *et al.*, “Underlying Event properties in pp collisions at $\sqrt{s} = 13$ TeV”, *JHEP* **04** (2020) 192, arXiv:1910.14400 [nucl-ex].
- [55] ALICE Collaboration, “Underlying-event properties in pp and p–Pb collisions at $\sqrt{s_{NN}} = 5.02$ TeV”, arXiv:2204.10389 [nucl-ex].
- [56] ALICE Collaboration, K. Aamodt *et al.*, “The ALICE experiment at the CERN LHC”, *JINST* **3** (2008) S08002. <https://iopscience.iop.org/article/10.1088/1748-0221/3/08/S08002>.
- [57] ALICE Collaboration, B. Abelev *et al.*, “Performance of the ALICE Experiment at the CERN LHC”, *Int. J. Mod. Phys.* **A29** (2014) 1430044, arXiv:1402.4476 [nucl-ex].
- [58] J. Alme *et al.*, “The ALICE TPC, a large 3-dimensional tracking device with fast readout for ultra-high multiplicity events”, *Nucl. Instrum. Meth.* **A622** (2010) 316–367, arXiv:1001.1950 [physics.ins-det].
- [59] ALICE Collaboration, A. Akindinov *et al.*, “Performance of the ALICE Time-Of-Flight detector at the LHC”, *Eur. Phys. J. Plus* **128** (2013) 44.
- [60] ALICE Collaboration, J. Adam *et al.*, “Determination of the event collision time with the ALICE detector at the LHC”, *Eur. Phys. J. Plus* **132** (2017) 99, arXiv:1610.03055 [physics.ins-det].
- [61] ALICE Collaboration, P. Cortese *et al.*, “ALICE technical design report on forward detectors: FMD, T0 and V0”, (2004) CERN–LHCC–2004–025.

- [62] P. Skands *et al.*, “Tuning PYTHIA 8.1: the Monash 2013 Tune”, *Eur. Phys. J. C* **74** (2014) 3024, arXiv:1404.5630 [hep-ph].
- [63] **GEANT4** Collaboration, S. Agostinelli *et al.*, “GEANT4—a simulation toolkit”, *Nucl. Instrum. Meth. A* **506** (2003) 250–303.
- [64] J. Jaros *et al.*, “Nucleus-nucleus total cross sections for light nuclei at 1.55 and 2.89 GeV/c per nucleon”, *Phys. Rev. C* **18** (1978) 2273–2292.
- [65] A. Auce *et al.*, “Reaction cross sections for 38, 65, and 97 MeV deuterons on targets from ${}^9\text{Be}$ to ${}^{208}\text{Pb}$ ”, *Phys. Rev. C* **53** (1996) 2919–2925.
- [66] S. P. Denisov *et al.*, “Measurements of anti-deuteron absorption and stripping cross sections at the momentum 13.3 GeV/c”, *Nucl. Phys. B* **31** (1971) 253–260.
- [67] F. G. Binon *et al.*, “Absorption cross-sections of 25 GeV/c antideuterons in Li, C, Al, Cu and Pb”, *Phys. Lett. B* **31** (1970) 230–232.
- [68] C. Tsallis, “Possible Generalization of Boltzmann-Gibbs Statistics”, *J. Statist. Phys.* **52** (1988) 479–487.
- [69] **PHENIX** Collaboration, S. S. Adler *et al.*, “Dense-Medium Modifications to Jet-Induced Hadron Pair Distributions in Au+Au Collisions at $\sqrt{s_{\text{NN}}} = 200$ GeV”, *Phys. Rev. Lett.* **97** (2006) 052301, arXiv:nucl-ex/0507004.
- [70] **ALICE** Collaboration, “Production of pions, kaons and protons as a function of the transverse event activity in pp collisions at $\sqrt{s} = 13$ TeV”, *CERN Document Server* (2022) . <https://cds.cern.ch/record/2841993>.
- [71] **ALICE** Collaboration, “Enhanced deuteron coalescence probability in jets. Supplemental Material: a model based on PYTHIA 8 and simple nucleon coalescence”, *ALICE-PUBLIC-2022-019* (Nov, 2022) . <http://cds.cern.ch/record/2842026>.
- [72] C. Bierlich *et al.*, “A comprehensive guide to the physics and usage of PYTHIA 8.3”, arXiv:2203.11601 [hep-ph].
- [73] L. A. Dal and A. R. Raklev, “Alternative formation model for antideuterons from dark matter”, *Phys. Rev. D* **91** (2015) 123536, arXiv:1504.07242 [hep-ph]. [Erratum: *Phys.Rev.D* **92**, 069903 (2015), Erratum: *Phys.Rev.D* **92**, 089901 (2015)].